Structure of $In_xGa_{1-x}As/GaAs$ strained-layer superlattices

S. F. Cui, G. M. Wang, Z. H. Mai, W. Feng, and J. M. Zhou
Institute of Physics, Chinese Academy of Sciences, Beijing 100080, China
(Received 16 March 1993; revised manuscript received 11 May 1993)

The cross-hatched morphology in $In_xGa_{1-x}As/GaAs$ strained-layer superlattices was shown by x-ray anomalous topography to be composed of edge-type dislocations running in two orthogonal ⟨110⟩ directions with their $\frac{1}{2}a\langle 110\rangle$ Burgers vector in the (001) growth plane. A type of stereoscopic topograph showed that the misfit dislocations were located over the whole superlattice and were stacked in columns along the surface normal. Based on a series of experimental results a relaxed growth mechanism for $In_xGa_{1-x}As/GaAs$ superlattices is proposed.

I. INTRODUCTION

Cross-hatched morphology (CHM) has been commonly noticed in strained III-V semiconductor films. The CHM has been observed by means of Nomarski interference, x-ray topography, TEM, cathodoluminescence, and photoluminescence in $Ga_{1-x}Al_xAs_{1-y}P_y/GaAs/Ga_{1-x}Al_xAs_{1-y}P_y$, or $Ga_{1-x}Al_xAs/Ga_{1-y}In_yAs/Ga_{1-x}Al_xAs$ laser structures,[1] $GaAs_{1-x}P_x/GaAs$,[2] $In_xGa_{1-x}As/GaAs$[3] or $GaAs/In_xGa_{1-x}As$ (Ref. 4) epilayers and $In_xGa_{1-x}As/GaAs$ strained-layer superlattices (SLS's).[5] Different kinds of explanations for the CHM have been proposed by the authors based on their own observations. Some models introduced, such as misfit dislocations,[1,3,4] lattice strains,[5,6] and disturbed growth,[2] were not consistent with one another. In particular, few results about the CHM were presented for the SLS. The crystal defects in III-V heterostructures were recently reviewed,[7] which did not involve superlattices.

In Sec. III, we report on x-ray topographic examinations of $In_xGa_{1-x}As/GaAs$ SLS's. It shows that the cross-hatched patterns in $In_xGa_{1-x}As/GaAs$ SLS's are misfit dislocations running in two orthogonal ⟨110⟩ directions in the (001) growth plane. Both of them are characterized as edge-type dislocations with $\frac{1}{2}a\langle 110\rangle$ Burgers vectors in the same plane. It was surprising that we observed the diffraction contrasts of cleavage planes of the SLS sample. This is evidence that the misfit dislocations are generated successively during the growth of the SLS sample and packed in columns perpendicular to the (001) growth plane. It might be considered that this successive generation and ordered distribution of the misfit dislocations originates from the interaction between the dislocations and the growth processes of the SLS.

In Sec. IV we summarize the structure of the $In_xGa_{1-x}As/GaAs$ SLS's studied.

II. EXPERIMENT

The samples of $In_xGa_{1-x}As/GaAs$ SLS's used in the experiments were grown on a GaAs substrate by molecular-beam epitaxy (MBE). The growth temperature was 520 °C. The nominal structure of the SLS samples were 150 or 100 periods of 70-Å $In_{0.04}Ga_{0.96}As$ and 250-Å GaAs with about a 1-μm GaAs buffer layer and a 3-μm GaAs capping layer, respectively. In order to eliminate the influence of the capping layer on the reflection topographs, a 150-period sample (denoted *A*) was etched to remove its capping layer. The other, unetched sample was denoted *B*. Another 100-period sample (denoted *C*) was etched to remove a portion of its capping layer. The synchrotron radiation experiments on sample *A* were performed at 4*W*1A beam line of the Beijing Synchrotron Radiation Facilities (BSRF). 1.59-Å monochromatic radiation was obtained from the 004 Bragg reflection on a silicon (001) crystal. A laboratory computer-controlled double-crystal diffractometer was also used to record rocking curves with Cu $K\alpha_1$ 004 reflection from a (001) GaAs crystal. To examine directly the "x-ray strains"[8] which represent the mismatch ($\epsilon^{\parallel}=\Delta a/a_0$) in interface planes, x-ray grazing incidence diffraction (GID) under total external reflection conditions was performed on an instrument previously described.[9] To probe the compositional inhomogeneity in the samples, a narrow scanning was performed on a Perkin-Elmer PH1 610 scanning Auger microprobe and energy dispersive spectra (EDS) were recorded on a Hitachi S570 scanning electron microscope (SEM) for samples *A* and *B*.

III. THE CROSS-HATCHED MORPHOLOGY

It has not been clear that the signal of In atoms on sample *A* was detected neither by scanning Auger spectrum nor by EDS. Any inhomogeneous distribution of Ga and As was not found within instrument accuracy while scanning the sample along the surface for 360 μm.

Figure 1 shows the 220 reflection for sample *A* measured by GID with different penetration depths. As is well known, this method measures mean "x-ray stains" $\epsilon^{\parallel}$. This means if there exist tensile and compressive strains in the samples simultaneously, net "x-ray strains" can be detected by GID.

The experimental Bragg diffraction peaks are significantly broader than those predicted theoretically[12] (9.6″ for GaAs 004 reflection). Table I lists the full widths at half maximum (FWHM's) for these three samples. In the determinations, the reference and the sample

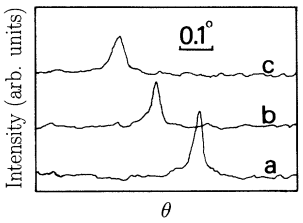

FIG. 1. Grazing incidence diffraction for sample A with grazing angle Φ (degree). (a) $\Phi=0.2$; (b) $\Phi=0.3$; and (c) $\Phi=0.4$ and 220 (reflection).

were carefully set up to ensure that the diffraction planes of the reference and the sample were vertical. Under these conditions the broadened Bragg peaks diffraction arises principally from the variation in tilts and dilations of the crystal lattice due to its dislocation structure.[10]

Figures 2(a) and 2(b) show 224 reflection topographs of sample A taken at the zeroth-order peak of the SLS and the substrate peak, respectively, and Fig. 3 is the same for sample C. The exposure time on Kodak films was 60 min. Because their strain field extends into the substrate, extended defects in the SLS are also imaged in the topographs taken at the substrate peak, while in the topographs taken at the zeroth-order peak the whole SLS is recorded. In Figs. 2 and 3 one can see the orthogonal striations running parallel to the [110] and [$\bar{1}$10] directions, respectively. To investigate the properties of these striations, we took a series of x-ray topographs based on the invisibility criteria of dislocations: $\mathbf{g}\cdot\mathbf{b}=0$ and $\mathbf{g}\cdot\mathbf{b}\times\mathbf{u}=0$ (where $\mathbf{g}$ is scattering vector, $\mathbf{b}$ the Burgers vector, and $\mathbf{u}$ the unit vector of dislocations). The x-ray topographs were taken under anomalous transmission conditions using Cu $K\alpha_1$ radiation ($\mu t=17$, where μ is the linear absorption constant and t the sample thickness). The back side of the substrate was polished and a 224 reflection topograph was taken to confirm its perfection before taking the transmission topographs. Figures 4(a) and 4(b) are the 220 and $\bar{2}20$ anomalous transmission topographs of sample A, respectively, taken with the SLS as the exit for the x-rays, while for Fig. 4(c) the $\bar{2}\,\bar{2}0$ topograph was taken with the substrate as the exit for the x-ray. It is evident that the striations running in the [110] direction disappear in the 220 transmission topograph.

Similar invisibility was observed in $\bar{2}20$ transmission topograph, but not in 004, 0$\bar{4}$4, 044, and 404 diffraction. Figures 5(a) and 5(b) are the 004 and 0$\bar{4}$4 reflection topographs, respectively. According to the criterion of dislocations, both the striations parallel to [110] and [$\bar{1}$10] are edge-type dislocations with Burgers vectors in [$\bar{1}$10] and [110] directions, respectively.

TABLE I. FWHM's (sec of arc).

Sample	004		440 (GID)
	Substrate	SLS	SLS
A	69	85	82
B	63	63	
C	71	55	55

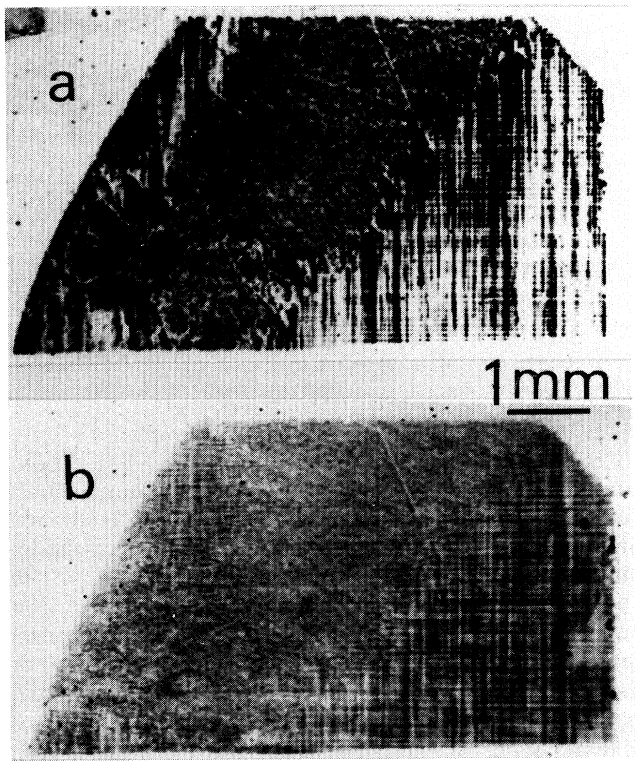

FIG. 2. Synchrotron radiation x-ray topographs of sample A taken at (a) the zeroth-order peak of the SLS; and (b) the substrate peak.

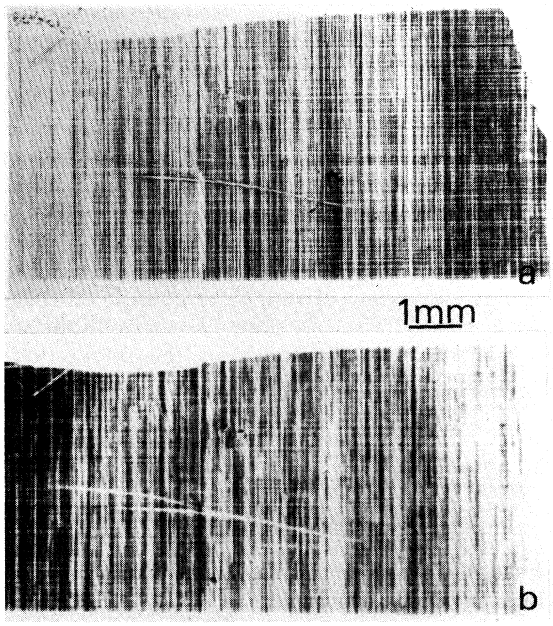

FIG. 3. Synchrotron radiation x-ray topographs for sample C taken at (a) the zeroth-order peak of the SLS; and (b) the substrate peak.

It is interesting to see that in addition to the striations in the (001) growth plane, other striations (see region *C* of Fig. 4) which obeyed the same extinction law were observed in the cleavage planes of sample *A*. Their contrasts are uniform and superimposed by those on the (001) growth plane. The stereoscopic topographs provide us with evidence that the misfit dislocations distribute over the whole SLS and are packed in columns along the surface normal.

There are three possible types of misfit dislocations in the zinc-blende crystal: edge, mixed 60°, or screw-type dislocation. The edge-type dislocations parallel to [110] with the Burgers vector $\frac{1}{2}a$ [$\bar{1}$10] in the (001) growth plane might be induced by the reaction of two 60° dislocations with Burgers vectors $\frac{1}{2}a\langle 110\rangle$ inclined at the angle of 45° to the (001) growth plane: $\frac{1}{2}a[\bar{1}10]=\frac{1}{2}a[\bar{1}0\bar{1}]+\frac{1}{2}a[011]$, while the edge dislocations parallel to [$\bar{1}$10] are induced by the reaction $\frac{1}{2}a[110]=\frac{1}{2}a[101]+\frac{1}{2}a[01\bar{1}]$. The edge-type dislocations cannot glide because their Burgers vectors are in the (001) plane.

It is important to notice that the critical compositions x_c required to produce a plastic deformation in the interfaces of $In_xGa_{1-x}As/GaAs$ and $GaAs/In_xGa_{1-x}As$ epilayers are quite different even for the same epilayer thicknesses. It has been reported[4,11] that x_c is 0.114 for $In_xGa_{1-x}As/GaAs$ and 0.006 for $GaAs/In_xGa_{1-x}As$ when the thickness is 2 μm. $In_xGa_{1-x}As/GaAs$ SLS's consist only of the above two types of structures. This means that it will be easier to produce a plastic deformation in the interfaces of $GaAs/In_xGa_{1-x}As$ than in that of $In_xGa_{1-x}As/GaAs$ for an $In_xGa_{1-x}As/GaAs$ SLS. Figure 6 shows a schematic drawing of a proposed relaxed growth mechanism for two periods of an $In_xGa_{1-x}As/GaAs$ SLS, in which only an extra half plane of the dislocations parallel to [$\bar{1}$10] is shown. The relaxation might occur in the first $GaAs/In_xGa_{1-x}As$ in-

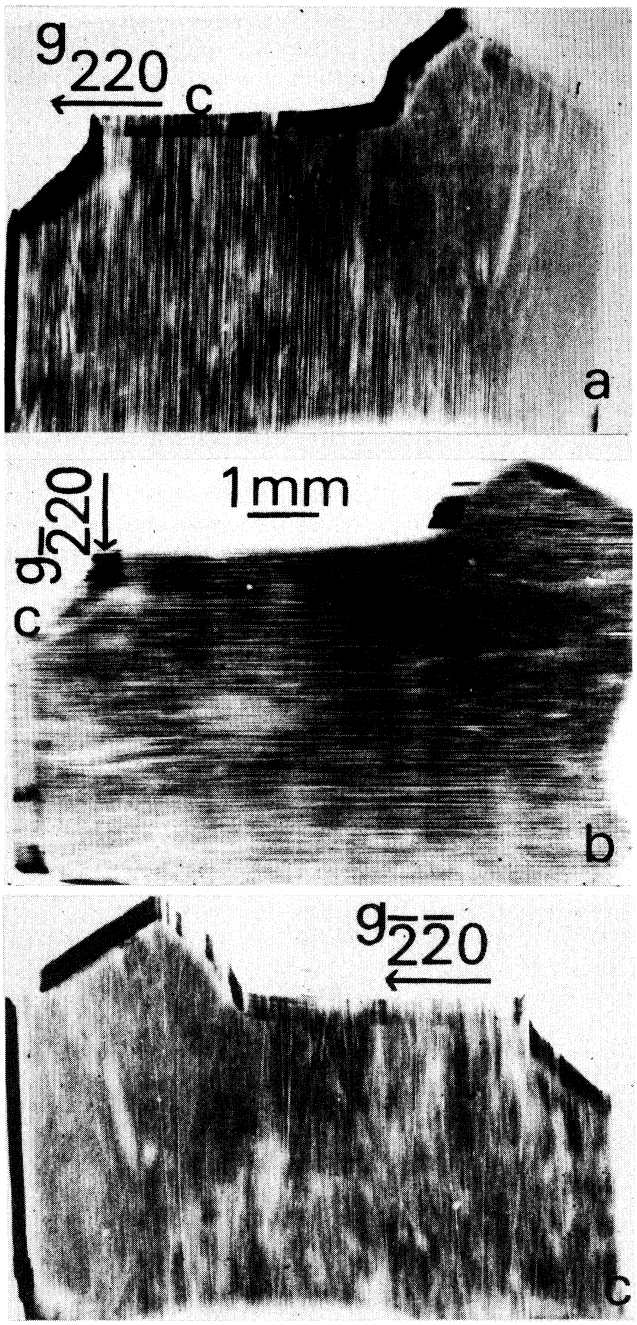

FIG. 4. Anomalous transmission topographs of sample *A*. (a) 220 reflection; (b) $\bar{2}20$ reflection; and (c) $\bar{2}\,\bar{2}0$ reflection.

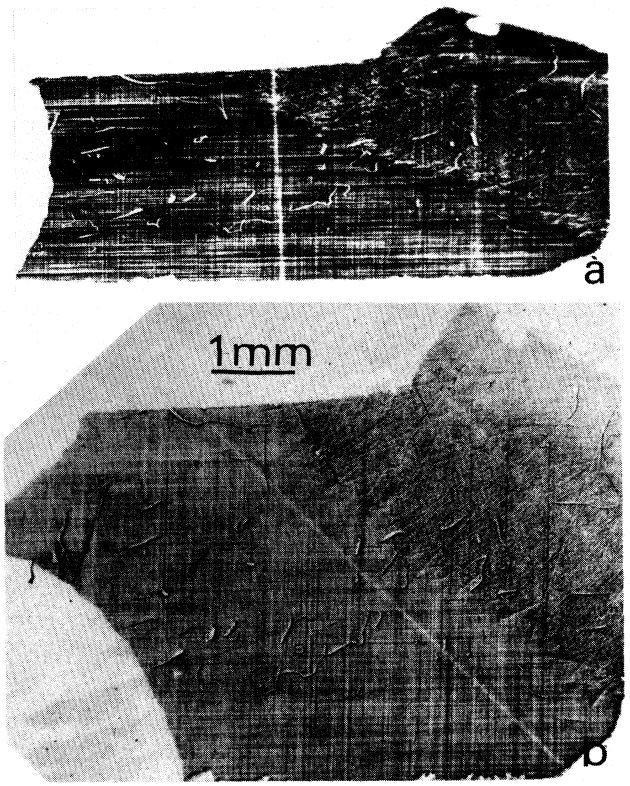

FIG. 5. Reflecting topographs of sample *A* taken at the zeroth-order peak of the SLS. (a) 004 reflection and (b) 0 $\bar{4}4$ reflection.

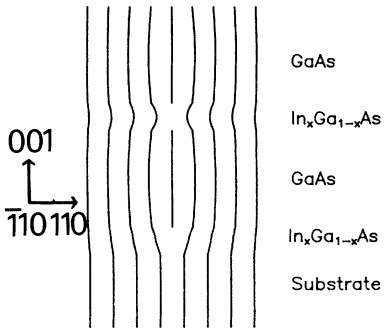

FIG. 6. The schematic drawing showing the generation of the dislocations in an $In_xGa_{1-x}As/GaAs$ SLS.

terface, and a positive edge dislocation should be produced, then compressive strains induced by the dislocation in the GaAs layer should make an increased migration rate of atoms at the growth surface. As a result, a relaxation in the next $In_xGa_{1-x}As/GaAs$ interface takes place and a negative edge dislocation is introduced. In the successive growth processes a series of dislocation dipoles are generated and packed in columns perpendicular to the (001) growth plane due to their immobility in this plane. However, the dislocation dipoles can move along a column by climbing.

Although the dislocation dipoles produce a compressive and a tensile strain alternatively in the interfaces of a SLS, they do not lead to an "x-ray strain" in the directions parallel to [110] or [$\bar{1}$10] in the (001) growth plane. In fact, we have not observed the "x-ray strains" in sample *A* by GID experiments with 220 (see Fig. 1) and 440 reflections for different penetration depths below the surface. Since [220] and [440] scattering vectors are parallel to Burgers vectors of dislocations, if there exists an "x-ray strain" in the SLS it should be detected.

It is worth noticing that not all the cross-hatched morphology in strained-layer semiconductors has a symmetry pattern in which two orthogonal striations are the same type of dislocations. For example, in $Ga_{1-x}Al_xAs/Ga_{1-x}In_xAs/Ga_{1-x}Al_xAs$ laser structures grown by liquid-phase epitaxy (LPE) on (001) GaAs substrates, the dislocations parallel to [110] have been determined to be edge-type ones with Burgers vectors in the (001) growth plane, while those parallel to [$\bar{1}$10] are 60°-type dislocations with their Burgers vector inclining an angle of 45° to the (001) plane.[1]

In addition, dark line defects were observed in $In_xGa_{1-x}As/GaAs$ SLS's by photoluminescence (PL) topography.[5] They were considered to originate from the locally deformed lattices by misfit stress, however, from our results the dark line defects are more likely induced by the orthogonal dislocation configurations described above rather than by elastic deformation.

IV. CONCLUSIONS

In summary, we reported the cross-hatched morphology in $In_xGa_{1-x}As/GaAs$ SLS's observed by synchrotron radiation topography. The orthogonal striations were determined by means of x-ray anomalous transmission topography to be edge-type dislocations with their Burgers vectors parallel to ⟨110⟩ directions in the (001) growth plane. The x-ray transmission topographs showed a stereoscopic image of dislocations in the SLS sample which provide us with a simple tool for identifying the CHM in superlattices. We proposed a model to explain the CHM in $In_xGa_{1-x}As/GaAs$ SLS's, that is, a series of dislocation dipoles successively generated due to the migration of mismatch strains, and are packed in columns perpendicular to the (001) growth plane because of the interaction between the misfit dislocations and the growth of the strained-layer superlattices.

ACKNOWLEDGMENT

This project was supported by the National Natural Science Foundation of China.

[1]W. J. Bartels and W. Nijman, J. Cryst. Growth **37**, 204 (1977).
[2]S. Kishino, M. Ogirima, and K. Kurata, J. Electrochem. Soc. **119**, 618 (1972).
[3]K. H. Chang, R. Gibala, D. J. Srolovitz, P. K. Bhattacharya, and J. F. Mansfield, J. Appl. Phys. **67**, 4093 (1990).
[4]Yang Baohua, Wang Yutian, Li Chengji, He Hongjia, Wang Zhanguo, and Lin Lanying, Chin. J. Semicond. **10**, 81 (1989).
[5]K. Iizuka, T. Yoshida, T. Suzuki, and H. Hirose, J. Cryst. Growth **111**, 429 (1991).
[6]R. A. Burmesiter, G. P. Pighini, and P. E. Greene, Trans. TMS-AIME **245**, 587 (1969).
[7]P. Franzosi, J. Cryst. Growth **126**, 109 (1993).
[8]S. F. Cui, Z. H. Mai, C. Y. Wang, and L. S. Wu, Modern Phys. Lett. B **23**, 1591 (1991).
[9]S. F. Cui, Z. H. Mai, L. S. Wu, C. Y. Wang, and D. Y. Dai, Rev. Sci. Instrum. **62**, 2419 (1991).
[10]B. K. Tanner and D. K. Bowen, J. Cryst. Growth **126**, 1 (1993).
[11]Wang Yutian, Li Chengji, and Ren Qingyu, Chin. J. Semicond. **10**, 637 (1989).
[12]Z. H. Mai, C. G. He, and S. F. Cui, Acta Phys. Sin. **38**, 782 (1990).

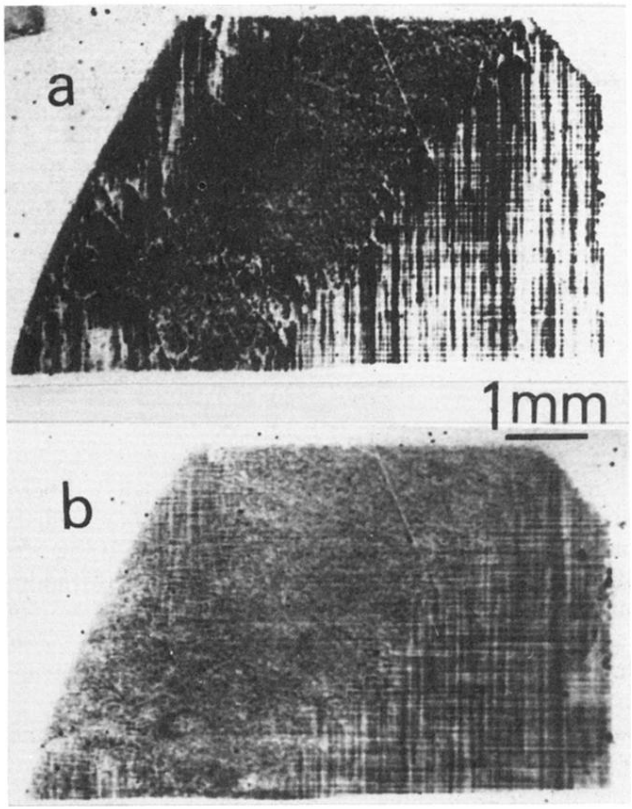

FIG. 2. Synchrotron radiation x-ray topographs of sample *A* taken at (a) the zeroth-order peak of the SLS; and (b) the substrate peak.

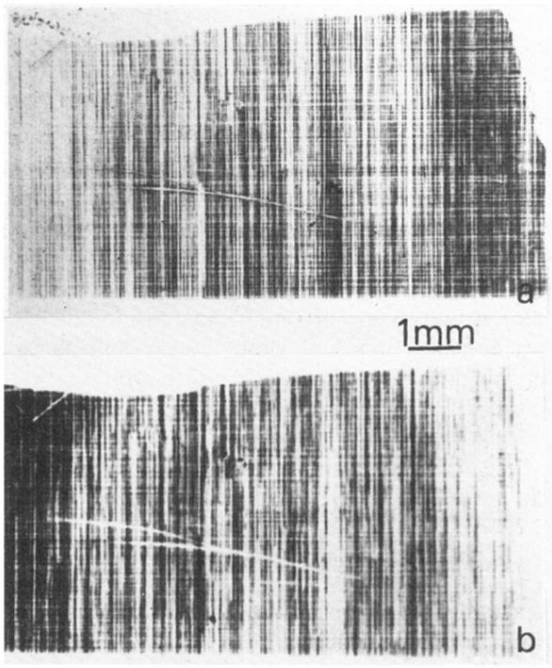

FIG. 3. Synchrotron radiation x-ray topographs for sample *C* taken at (a) the zeroth-order peak of the SLS; and (b) the substrate peak.

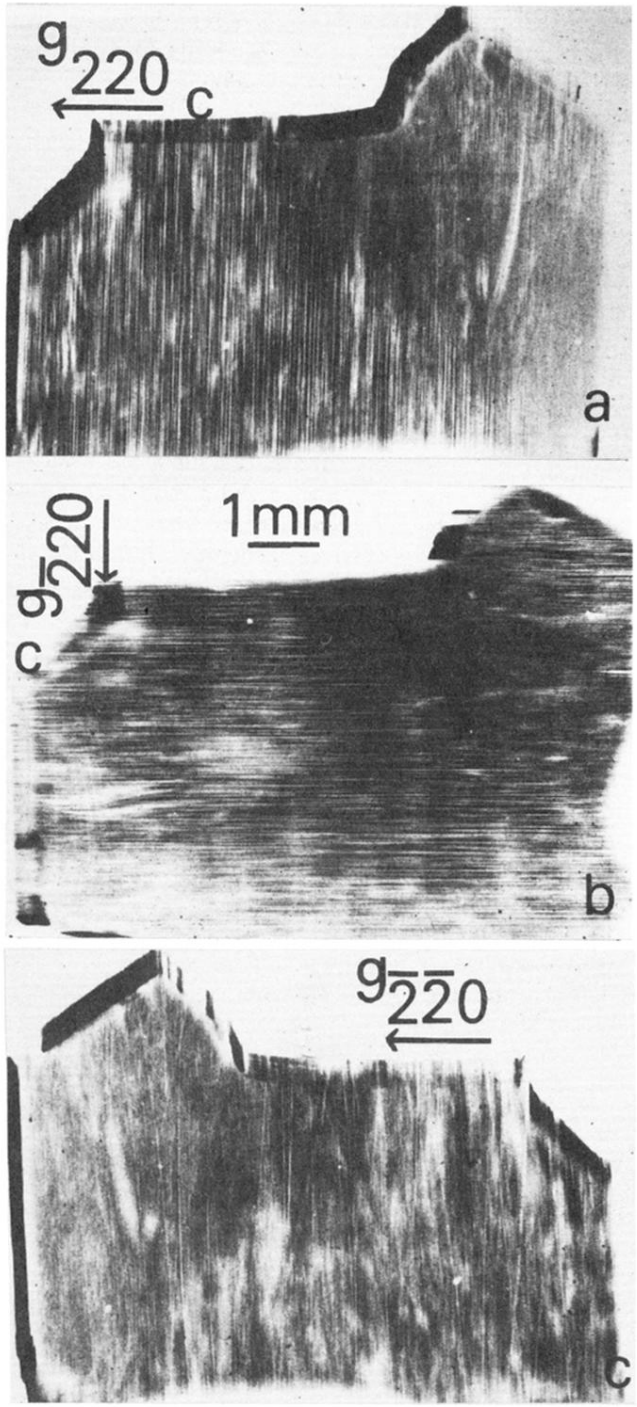

FIG. 4. Anomalous transmission topographs of sample *A*. (a) 220 reflection; (b) $\bar{2}20$ reflection; and (c) $\bar{2}\,\bar{2}0$ reflection.

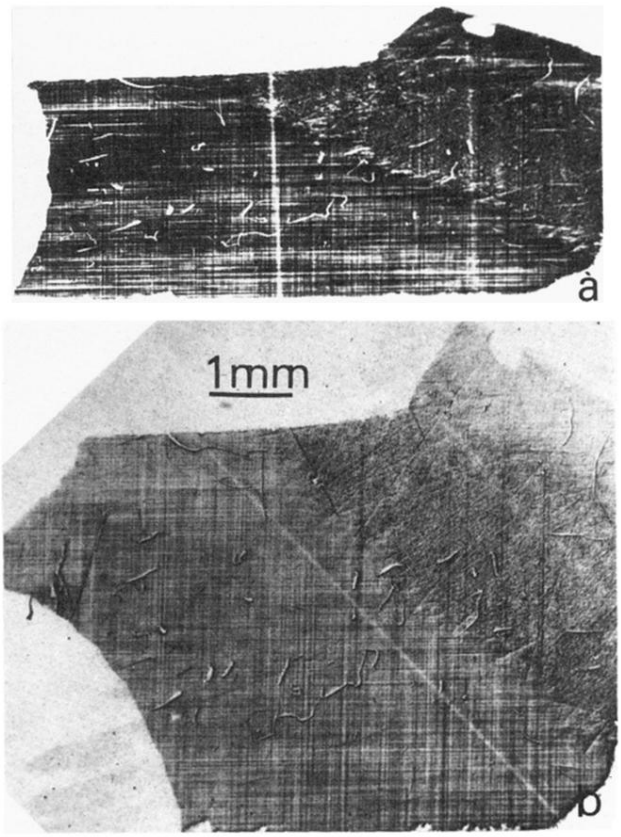

FIG. 5. Reflecting topographs of sample *A* taken at the zeroth-order peak of the SLS. (a) 004 reflection and (b) 0 $\bar{4}4$ reflection.